Electronic supplementary information

Significantly enhanced electron transport of nonfullerene acceptor in blend film with high hole mobility polymer of high molecular weight: thick-film nonfullerene polymer solar cells showing high fill factor †

Zhen Wang,[a] Haiying Jiang,[a] Xuncheng Liu,[a] Jiahao Liang,[a] Lianjie Zhang,[a] Lechi Qing,[a] Qian Wang,[a] Wei Zhang,[b] Yong Cao[a] and Junwu Chen*[,a,c]

[a]*Institute of Polymer Optoelectronic Materials & Devices, State Key Laboratory of Luminescent Materials & Devices, South China University of Technology, Guangzhou 510640, China. E-mail: psjwchen@scut.edu.cn*

[b]*School of Physics and Electronic Engineering, Guangzhou University, Guangzhou 510006, China*

[c]*South China Institute of Collaborative Innovation, Dongguan 523808, China*

Polymer Synthesis

The polymerization for Si25 polymers were carried out according to a previous report.[1] In a 50 mL two-neck round-bottom flask under argon protection, 4,7-bis(5-bromo-4-(5-(1,1,1,3,5,5,5-heptamethyltrisiloxan-3-yl)pentyl)thiophen-2-yl)-5,6-difluorobenzothiadiazole (161 mg, 0.15 mmol), 4,7-dibromo-5,6-difluoro[2,1,3]benzothiadiazole, 4,7-bis(5-bromo-4-(2-decyltetradecyl)thiophen-2-yl)-5,6-difluoro[2,1,3]benzothiadiazole (525 mg, 0.45 mmol), 5,5'-bis(trimethylstannyl)-2,2'-bithiophene (295 mg, 0.6 mmol), $Pd_2(dba)_3$ (11 mg), and tri(o-tolyl)phosphine (15 mg) were dissolved in chlorobenzene (10 mL). The solution was refluxed with vigorous stirring for 72 h. At the end of polymerization, a small amount of 2-tributylstannylthiophene was added as a monofunctional end-capping reagent to remove bromine end groups, and bromobenzene was added as a monofunctional end-capping reagent to remove trimethylstannum end group. The mixture was then poured into vigorously stirred methanol. The precipitated solid was placed in a Soxhlet thimble, and extracted consecutively

with methanol, ethyl acetate, acetone, chloroform, and chlorobenzene. Then the chlorobenzene fraction was concentrated, precipitated in methanol at room temperature, and then filtered and dried in vacuum at 50 ℃ for 2 days to give 614 mg of final Si25-H2 product as a black solid in a yield of 93%. Elemental analysis: calculated: C, 66.88%; H, 8.37%; N, 2.44%; S, 13.95%. Found: C, 66.83%; H, 8.42%; N, 2.31%; S, 13.65%. High temperature GPC (1,2,4-trichlorobenzene, 140 ℃): M_n, 105.6 Kg/mol; M_w/M_n, 2.14.

The polymerization for Si25-H1 was carried out similarly as that for Si25-H2, but with a higher amount of co-catalyst tri(o-tolyl)phosphine (22.5 mg) and a shorter polymerization time of 48 h. Si25-H1 was finally extracted with chlorobenzene, in a yield of 92%.. High temperature GPC (1,2,4-trichlorobenzene, 140 ℃): M_n, 98.6 Kg/mol; M_w/M_n, 2.32.

Si25-L was carried out similarly as that for Si25-H2, but with a very short polymerization time of 8 h. The Si25-H1 of low molecular weight was finally extracted with chloroform, in a yield of 86%. High temperature GPC (1,2,4-trichlorobenzene, 140 ℃): M_n, 12.7 Kg/mol; M_w/M_n, 2.13.

Fabrication and Characterization of Polymer Solar Cells (OSCs)

The device structure was ITO/ZnO/PFN-Br/Si-25:IEICO-4F (1:1.5 by weight)/MoO_3/Al. Patterned indium tin oxide (ITO)-coated glass with a sheet resistance of 15–20 ohm/square was cleaned by a surfactant scrub and then underwent a wet-cleaning process inside an ultrasonic bath that began with deionized water, followed by acetone and 2-propanol. A precursor solution of zinc acetate dehydrate in 2-methoxyethanol and a small amount of ethanolamine was spin-coated on ITO substrate, and then annealed at 200 ℃ for 40 min in air to form a 30 nm ZnO layer. The substrates were then transferred into a nitrogen-filled glove box. Afterward, around 10 nm PFN-Br layer (0.5 mg/mL in methanol, 2000 rpm) was spin-coated onto the ZnO layer. Active layer solutions (D/A ratio of 1:1.5) with different donor concentrations were prepared in CB with 0.5% (volume fraction) of 1-chloronaphthalene. Warm solutions (90 ℃) were then spin-coated onto the substrates and dried at 80 ℃ for 5 min. A 10 nm MoO_3 layer and a 100

nm Al layer were subsequently evaporated through a shadow mask to define the active area of the devices (5.7 mm^2) and form the top anode. The PCE was determined from *J*-*V* curve measurements (using a Keithley 2400 source meter unit) under a 1 sun, AM 1.5G spectrum from a solar simulator (Oriel model 91192; 1000 W m^{-2}). The solar simulator illumination intensity was determined using a monocrystal silicon reference cell (Hamamatsu S1133, with KG-5 visible color filter) calibrated by the National Renewable Energy Laboratory (NREL). Integrated J_{sc} values were obtained with EQE under the AM 1.5G solar spectrum, which agreed with the measured value to within 5%.

Space-Charge Limited Current (SCLC) Measurement

Hole-only and electron-only devices were fabricated to measure the hole and electron mobilities of active layers using the space charge limited current (SCLC) method with hole-only device of ITO/PEDOT:PSS/Active layer/MoO_3/Al and electron-only device of ITO/ZnO/Active layer/PFN-Br/Al. The mobilities (μ) were determined by fitting the dark current to the model of a single carrier SCLC, described by the equation:

$$J = \frac{9}{8}\varepsilon_0\varepsilon_r\mu\frac{V^2}{d^3}$$

where *J* is the current, ε_0 is the permittivity of free space, ε_r is the material relative permittivity, *d* is the thickness of the active layer, and *V* is the effective voltage. The effective voltage can be obtained by subtracting the built-in voltage (V_{bi}) and the voltage drop (V_s) from the substrate's series resistance from the applied voltage (V_{appl}), $V = V_{appl} - V_{bi} - V_s$. The mobility can be calculated from the slope of the $J^{1/2} \sim V$ curves.

Time-Resolved Photoluminescence Measurements (TRPL)

TRPL was measured in a setup described in a previous report.[2] The frequency-doubled (400 nm) *s*-polarized light from Ti:Sapphire fs laser (Spectra-Physics Tsunami, MKS instruments Inc., Andover, MA, USA) with a pulse duration of ~100 fs was used for excitation. PL was collected and focused on the input slit of a spectrograph (Model 250is, Chromex Inc., Albuquerque, NM, USA) by two quartz plano-convex lenses. The output of the spectrograph

was projected onto the input slit of the streak camera (Hamamatsu C6860, Hamamatsu Photonics, Hamamatsu, Japan). All samples were kept in N_2 and were measured at room temperature. Efforts were taken to keep the alignment of the experimental set-up the same for all the samples studied.

Grazing Incidence Wide-Angle X-ray Scattering (GIWAXS) Characterization

GIWAXS measurements were carried out on a Xenocs Xeuss 2.0 system with an Excillum MetalJet-D2 X-ray source operated at 70.0 kV, 2.8570 mA, and a wavelength of 1.341 Å. The grazing-incidence angle was set at 0.20 °. Scattering pattern was collected with a Dectris Pilatus3R 1M area detector.

Atomic Force Microscopy and Transmission Electron Microscopy

Tapping-mode atomic force microscopy (AFM) images were obtained using a Nano Scope NS3A system (Digital Instrument) to observe the surface morphology of active layers. Transmission electron microscopy (TEM) images were obtained using JEM-2100F with an accelerating voltage of 30 kV.

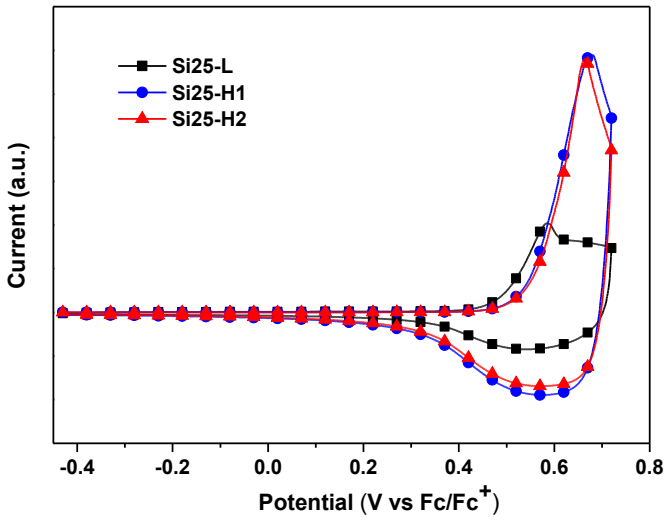

Fig. S1. Cyclic voltammetry curves of the three Si25 polymers.

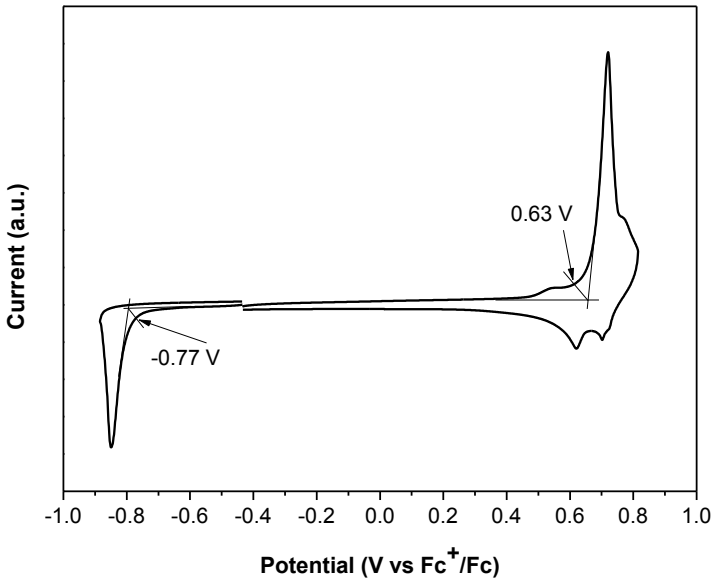

Fig. S2. Cyclic voltammetry curves of the IEICO-4F.

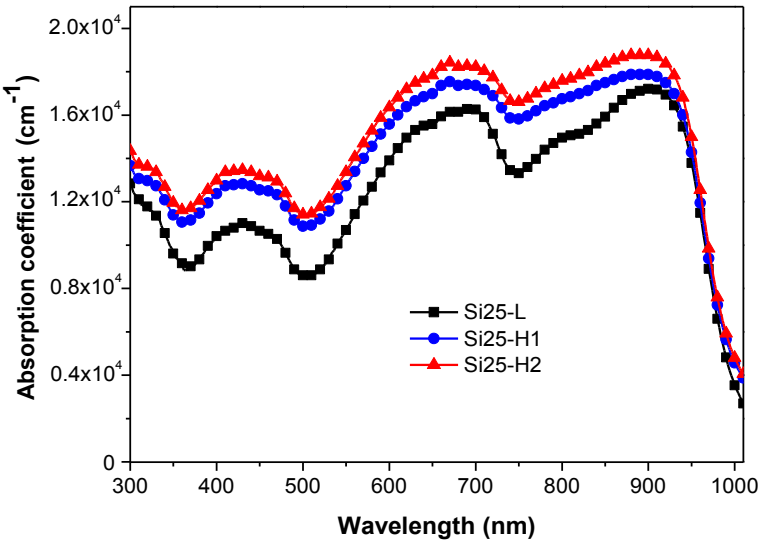

Fig. S3. The absorption coefficients of Si25:IEICO-4F blend films (D/A ratio of 1:1.5).

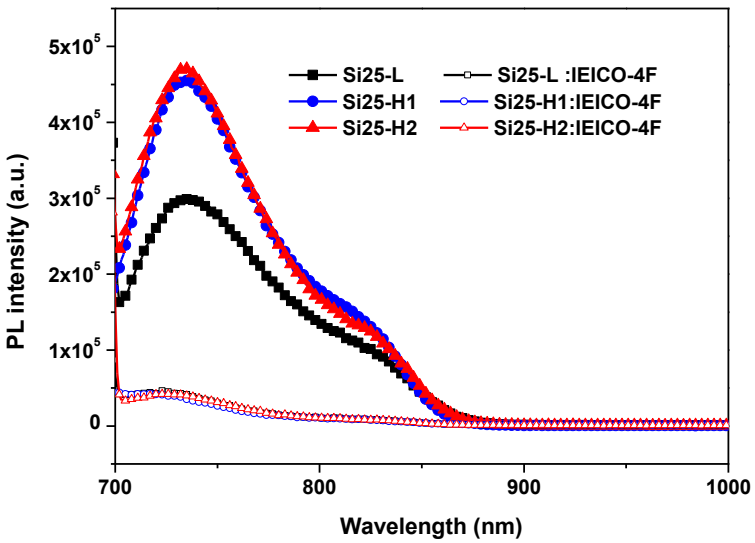

Fig. S4. PL spectra of the 320 nm thick pristine and blend films of the three Si25 polymers, under excitation wavelength of 688 nm. The PL quenching extents are of 84.7%, 90.7%, and 91.0% for the Si25-L, Si25-H1, and Si25-H2 based blend films, respectively.

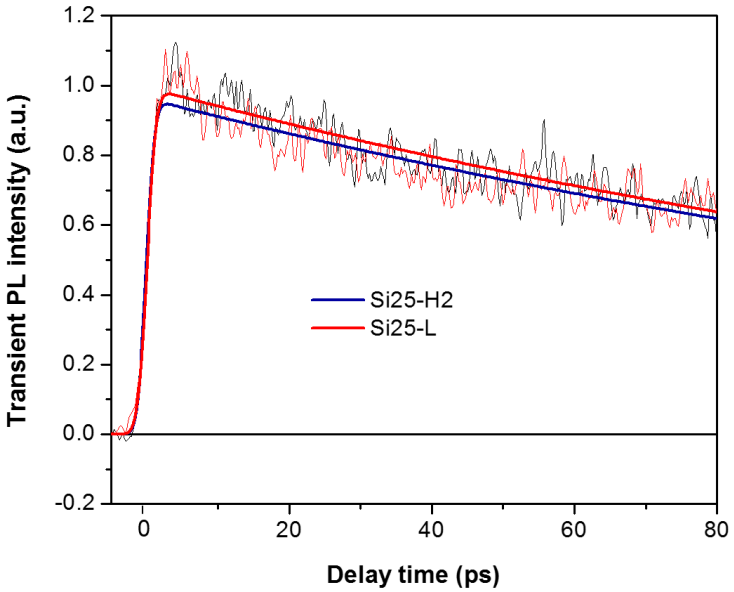

Fig. S5. Transient PL kinetics of pristine films of Si25-L and Si25-H2 at 750 nm after photoexcitation at 400 nm. The bold solid lines are based on mono-exponential fitting. The fitted lifetime values for the Si25-L and Si25-H2 are of 180.5 and 179.9 ps, respectively.

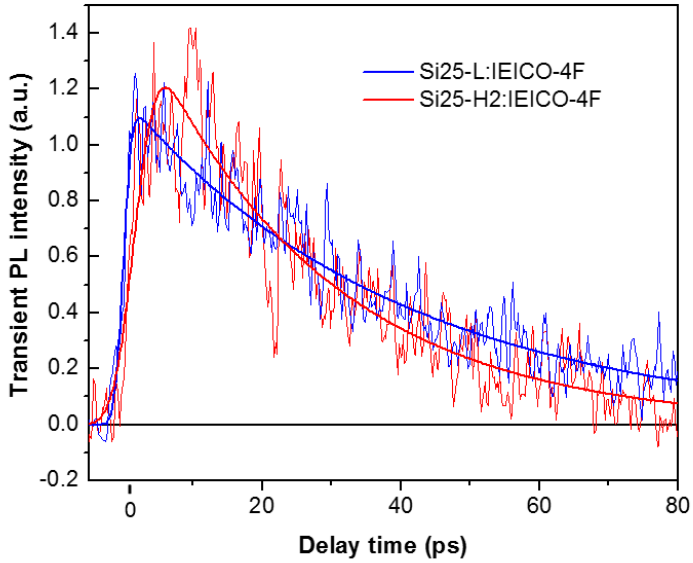

Fig. S6. Transient PL kinetics of the 320 nm thick Si25-L and Si25-H2 based blend films at 970 nm after photoexcitation at 400 nm. The bold solid lines are based on mono-exponential fitting.

Table S1. The fitted lifetime ($\bar{\tau}$) values for the 320 nm thick Si25-L and Si25-H2 based blend films. The mono- and bi-exponential fittings correspond to probe wavelengths of 970 and 750 nm, respectively.

Blend film	Probe light (nm)	A_1	τ_1(ps)	A_2	τ_2(ps)	$\bar{\tau}$(ps)
Si25-L:IEICO-4F	750	0.82	5.3	0.59	45.8	22.2
Si25-H2:IEICO-4F	750	1.08	3.3	0.57	21.3	9.52
Si25-L:IEICO-4F	970	1.17	39.8			39.8
Si25-H2:IEICO-4F	970	1.47	26.3			26.3

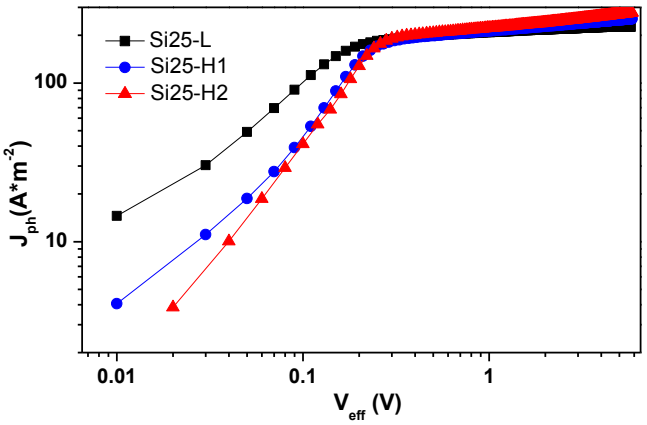

Fig. S7. Photocurrent density (J_{ph}) versus effective voltage (V_{eff}) characteristics of the PSCs based on 320 nm thick Si25:IEICO-4F active layers. The V_{eff} is gained by subtracting the applied voltage from the voltage where J_{ph} is zero.

Table S2. The summarized J_{sc}, J_{sat}, P(E,T), and G_{max} of the PSCs based on 320 nm thick Si25:IEICO-4F active layers.

device	J_{sc} (mA/cm^2)	J_{sat}[a] (mA/cm^2)	P(E,T)[b] (%)	G_{max}[c] ($m^{-3}s^{-1}$)
Si25-L	19.34	22.56	85.70	4.7×10^{27}
Si25-H1	23.98	25.42	94.30	5.3×10^{27}
Si25-H2	26.44	27.83	95.00	5.4×10^{27}

a) The saturation current density with V_{eff} = 2 V in Figure S4. b) The charge dissociation probability determined from the ratio of J_{ph}/J_{sat}. c) The maximum exciton generation rate according to $G_{max} = J_{sat}/qL$, where q is elementary charge and L is the thickness of active layer.

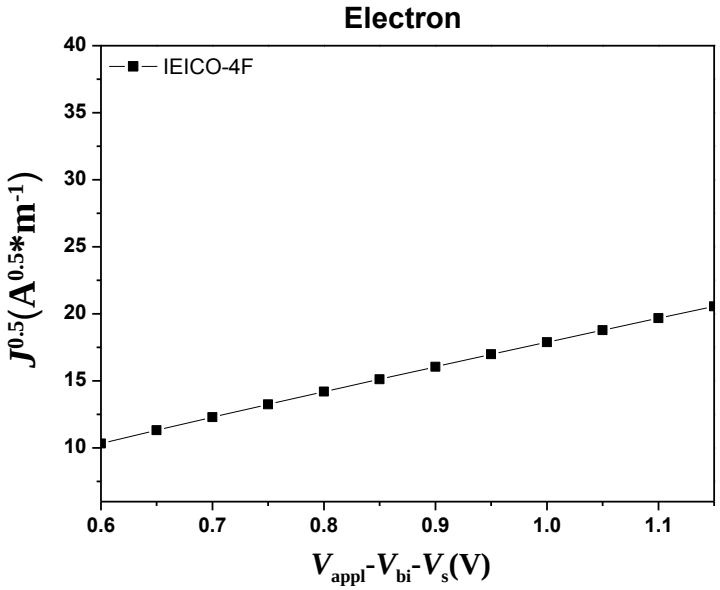

Fig. S8. SCLC $J^{0.5}$-V characteristics of a100 nm thick pristine IEICO-4F film in an electron-only device of ITO/ZnO/IEICO-4F film/PFN-Br/Al.

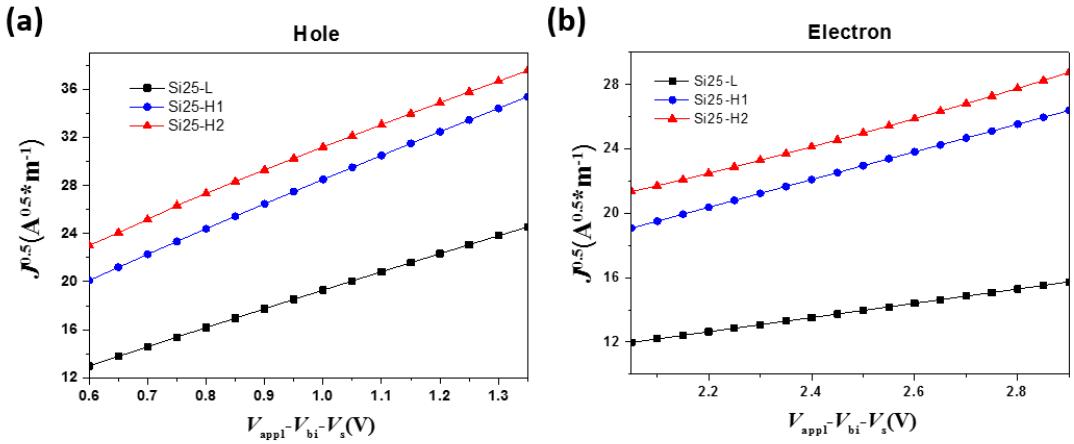

Fig. S9. SCLC $J^{0.5}$-V characteristics of the 320 nm thick Si25:IEICO-4F blend films in (a) hole-only and (b) electron-only devices, with device configurations of ITO/PEDOT:PSS/blend film/MoO_3/Al and ITO/ZnO/blend film/PFN-Br/Al, respectively.

Table S3. Packing parameters for IEICO-4F, Si25-L, Si25-H1, and Si25-H2 neat films and their BHJ blend films, based on GIWAXS measurements

sample	(100) peaks for donor (OOP)/acceptor (IP)			OOP (010) peaks		
	Position ($Å^{-1}$)	*d*-spacing (Å)	CL (Å)	Position ($Å^{-1}$)	π-π distance (Å)	CL (Å)
IEICO-4F	/0.31	/20.26	/127.87	1.84	3.41	38.91
Si25-L	0.25/	25.12/	162.72/	\	\	\
Si25-H1	0.26/	24.15/	94.02/	\	\	\
Si25-H2	0.27/	23.26/	123.13/	\	\	\
Si25-L:IEICO-4F	0.25/0.32	25.12/19.63	129.26/141.17	1.84	3.41	37.91
Si25-H1:IEICO-4F	0.26/0.33	24.15/19.03	63.78/127.99	1.84	3.41	38.06
Si25-H2:IEICO-4F	0.27/0.34	23.26/18.47	85.04/128.46	1.84	3.41	40.25

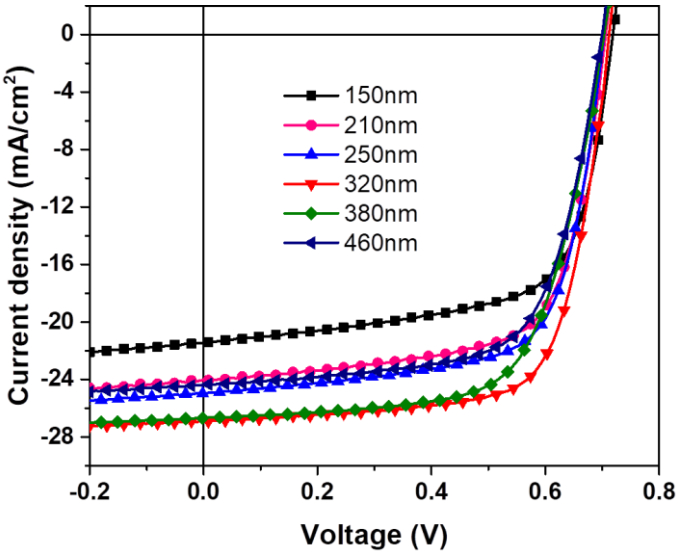

Fig. S10. *J-V* characteristics of Si25-H2:IEICO-4F based PSCs with different active layer thicknesses.

Table S4. Photovoltaic performances of Si25-H2:IEICO-4F based PSCs with different active layer thicknesses.

Thickness (nm)	V_{oc} (V)	J_{sc} (mA cm^{-2})	FF (%)	PCE[a)] (%)
150	0.72	21.44	66.28	10.26 (9.92)
210	0.71	24.04	68.57	11.58 (11.19)
250	0.71	24.95	68.80	12.02 (11.84)
320	0.70	26.87	70.15	13.20 (12.88)
380	0.70	26.72	68.41	12.79 (12.43)
460	0.70	24.39	66.84	11.45 (11.24)

a) The averaged PCE is given in the parenthesis.

References.

1. X. Liu, L. Nian, K. Gao, L. Zhang, L. Qing, Z. Wang, L. Ying, Z. Xie, Y. Ma, Y. Cao, F. Liu and J. Chen, *J. Mater. Chem. A*, 2017, **5**, 17619.

2. W. Zhang, S. Lehmann, K. Mergenthaler, J. Wallentin, M. T. Borgström, M.-E. Pistol and A. Yartsev, *Nano Lett.*, 2015, **15**, 7238.